This document is the accepted manuscript version of the following article:
Leresche, F., McKay, G., Kurtz, T., von Gunten, U., Canonica, S., & Rosario-Ortiz, F. L. (2019). Effects of ozone on the photochemical and photophysical properties of dissolved organic matter. Environmental Science and Technology, 53(10), 5622-5632. https://doi.org/10.1021/acs.est.8b06410

Effects of Ozone on the Photochemical and Photophysical Properties of Dissolved Organic Matter

Frank Leresche [⊥], Garrett McKay [⊥], Tyler Kurtz [⊥], Urs von Gunten [†,‡], Silvio Canonica [†] and Fernando L. Rosario-Ortiz [⊥,*]

[⊥]Department of Civil, Environmental and Architectural Engineering, University of Colorado, Boulder, Colorado 80309, United States

[†]Eawag, Swiss Federal Institute of Aquatic Science and Technology, Überlandstrasse 133, CH-8600 Dübendorf, Switzerland

[‡]School of Architecture, Civil and Environmental Engineering (ENAC), Ecole Polytechnique Fédérale de Lausanne (EPFL), CH-1015 Lausanne, Switzerland

[*] Corresponding author: Fernando.rosario@colorado.edu

Abstract

This study focused on the effects of ozonation on the photochemical and photophysical properties of dissolved organic matter (DOM). Upon ozonation, a decrease in DOM absorbance was observed in parallel with an increase in singlet oxygen ($^1O_2$) and fluorescence quantum yields (Φ_{1O2} and Φ_F). The increase in Φ_{1O2} was attributed to the formation of quinone-like moieties during ozonation of the phenolic moieties of DOM, while the increase in Φ_F can be explained by a significant decrease in the internal conversion rate of the first excited singlet state of the DOM (^{1}DOM*). It is a consequence of an increase in the average energy of the first electronic transition ($S_1 \rightarrow S_0$) that was assessed using the wavelength of maximum fluorescence emission ($\lambda_{F,max}$). Furthermore, ozonation did not affect the ratio of the apparent steady-state concentrations of excited triplet DOM (^{3}DOM*) and $^1O_2$, indicating that ozonation does not affect the efficiency of $^1O_2$ production from ^{3}DOM*. The consequences of these changes for the phototransformation rates of micropollutants in surface waters were examined using photochemical model calculations. The decrease in DOM absorbance caused by ozonation leads to an enhancement of direct photolysis rates due to the increased transparency of the water. Rates of indirect photolysis induced by $^1O_2$ and ^{3}DOM* slightly decrease after ozonation, whereas the increases in water transparency, Φ_{1O2} and Φ_F are overcompensated by the decrease in DOM absorbance.

Graphical abstract

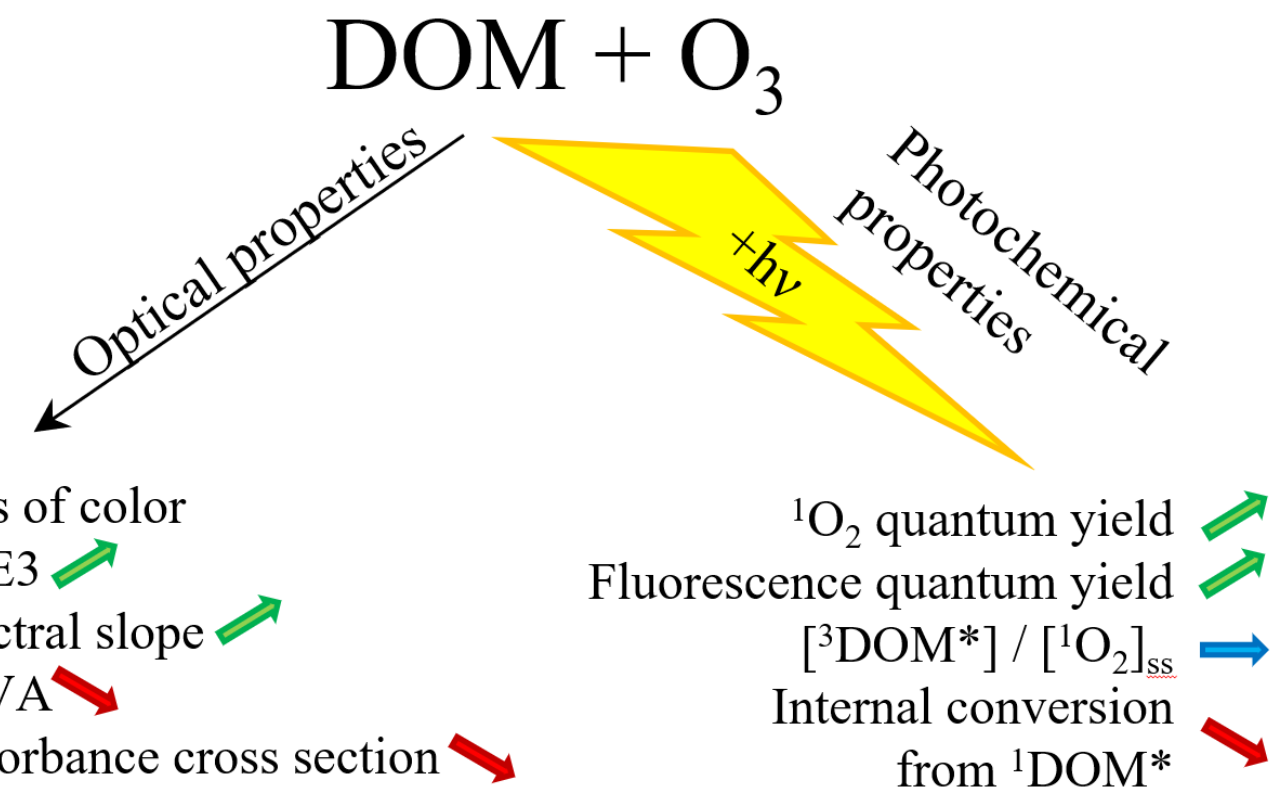

Introduction

The photophysical and photochemical properties of dissolved organic matter (DOM) are of interest due to their control on many important processes in environmental chemistry, including contaminant fate and optical properties of natural systems.[1, 2] The photophysical properties of DOM refer to the absorption of light and to the processes involved in the decay of the excited chromophores within DOM to the ground electronic state, including fluorescence. The photochemistry of DOM refers to chemical reactions resulting from the absorption of light, including the formation of reactive intermediates such as the hydroxyl radical ($^{\bullet}OH$), singlet oxygen ($^1O_2$) the superoxide radical anion ($O_2^{\bullet-}$) and excited triplet states of the DOM ($^3DOM^*$).[3-5]

In the frame of this study, we discuss the relevant links between photophysical and photochemical processes of DOM based on a simplified model represented in Scheme 1, which is similar to previously reported schemes[2, 4-6] (a more detailed analysis is provided in the Supporting Information (SI), Text S5). The first step for the formation of reactive intermediates such as $^1O_2$ and $^3DOM^*$ is the absorption of a photon that triggers a change in the electronic configuration of a chromophore within DOM, with an electron being promoted to one of the free electronic molecular orbitals and then undergoing a very fast relaxation to the first excited singlet state of the DOM ($^1DOM^*$). This $^1DOM^*$ can be a strong oxidant, but due to its very short lifetime (50 ps to a few ns),[7] tends to not react with species that are not in close proximity as diffusion is very limited at this timescale. The main decay pathway of $^1DOM^*$ is internal conversion (IC), a non-radiative transition to the ground state of DOM, but $^1DOM^*$ can also undergo radiative decay (fluorescence) or intersystem crossing (ISC), which is another non-radiative transition, to give a $^3DOM^*$ that can

also be a strong oxidant and the precursor of $^1O_2$ in surface waters.[4] $^{\bullet}OH$ is produced from DOM through a variety of pathways (not shown in Scheme 1 for simplicity), including the photo-Fenton reaction.[8, 9] $^1O_2$ is a very selective oxidant that is involved in the transformation of electron-rich phenols, anilines, some antibiotics of the sulfonamide class,[10] the pharmaceutical cimetidine,[11] several amino acids and can also react with bacteria and viruses thereby influencing the chemical and microbiological quality of the water.[12-14]

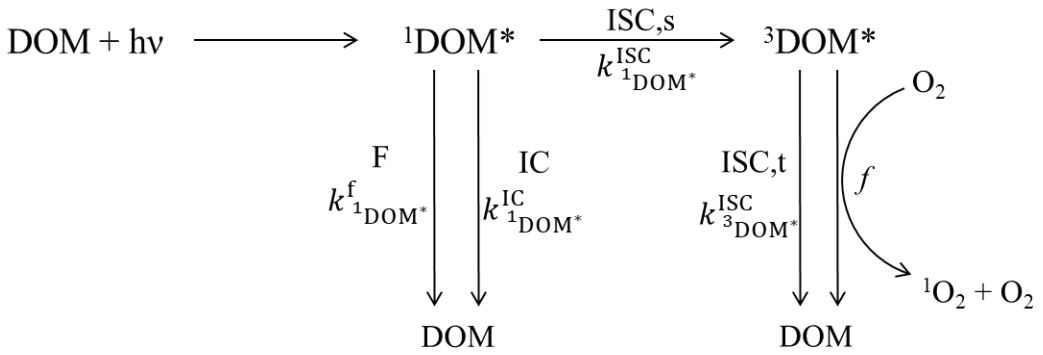

Scheme 1. Mechanisms for the formation and decay of excited singlet and triplet state dissolved organic matter (^{1}DOM* and ^{3}DOM*, respectively) upon photon absorption of a chromophore of DOM. F and $k^f_{^1DOM^*}$, are the fluorescence and the fluorescence rate constant, respectively. IC and $k^{IC}_{^1DOM^*}$ are the internal conversion and internal conversion rate constant for ^{1}DOM*, respectively. ISC,s and $k^{ISC}_{^1DOM^*}$are the intersystem crossing (ISC) and the ISC rate constant, from ^{1}DOM*, respectively. Similarly, ISC,t and $k^{ISC}_{^3DOM^*}$are the ISC and the ISC rate constant, from ^{3}DOM* respectively. f is the efficiency factor of singlet oxygen ($^1O_2$) production from ^{3}DOM* (see also SI, eqs. S16 and S17).

Since DOM may be viewed as a mixture of chromophores with individual characteristics, the values of kinetic constants and quantum yields related to a specific photophysical or photochemical process are averages of the corresponding values of each individual DOM chromophore. They can be expressed by equations 1 – 3, with the rate constants defined as in Scheme 1. It should also be noted that the quantum yields are the results of competing pathways and that an increase or decrease in a rate constant would affect each quantum yield differently.

$$\Phi_{\mathrm{f}} = \frac{k^{\mathrm{f}}{}_{^1\mathrm{DOM}^*}}{k^{\mathrm{f}}{}_{^1\mathrm{DOM}^*} + k^{\mathrm{ISC}}{}_{^1\mathrm{DOM}^*} + k^{\mathrm{IC}}{}_{^1\mathrm{DOM}^*}} \quad (1)$$

$$\Phi\,{}^3\mathrm{DOM}^* = \frac{k^{\mathrm{ISC}}{}_{^1\mathrm{DOM}^*}}{k^{\mathrm{f}}{}_{^1\mathrm{DOM}^*} + k^{\mathrm{ISC}}{}_{^1\mathrm{DOM}^*} + k^{\mathrm{IC}}{}_{^1\mathrm{DOM}^*}} \quad (2)$$

$$\Phi\,{}^1\mathrm{O}_2 = \frac{k^{\mathrm{ISC}}{}_{^1\mathrm{DOM}^*}}{k^{\mathrm{f}}{}_{^1\mathrm{DOM}^*} + k^{\mathrm{ISC}}{}_{^1\mathrm{DOM}^*} + k^{\mathrm{IC}}{}_{^1\mathrm{DOM}^*}} \times \frac{f \times k^{\mathrm{q}}{}_{^3\mathrm{DOM}^*,\mathrm{O}_2}}{k^{\mathrm{q}}{}_{^3\mathrm{DOM}^*,\mathrm{O}_2} + k^{\mathrm{ISC}}{}_{^3\mathrm{DOM}^*}} \quad (3)$$

A current topic of interest in environmental chemistry is the relationship between DOM photophysics and photochemistry, specifically the relation between optical properties (i.e., absorbance and fluorescence) and the efficiency (i.e., quantum yields) of reactive intermediates formation. These intermediates are formed with quantum yields in the order of 0.5-5.5% for $^1O_2$, [15-22] 4-8% for ^{3}DOM* [23, 24] and <0.02% for $^{\bullet}$OH. [8, 25, 26] Quantum yields of reactive intermediates have been correlated to optical properties such as the *E2/E3* ratio (ratio of the absorbance values at the wavelengths of 250 nm and 365 nm), spectral slope (see eq. 4 for its definition), and specific ultraviolet absorbance (SUVA) for DOM samples of diverse provenance and character, indicating the role of DOM composition in determining photoreactivity.[16, 17, 27] While these optical parameters correlate with DOM composition, they do not describe fundamental DOM photophysical pathways. In addition, a positive correlation has been observed between quantum yields of reactive intermediates formation and fluorescence quantum yields (Φ_f). [18, 28] This observation can be linked to the influence of the internal conversion.[18, 28, 29] For example, a decrease in internal conversion rate will favor fluorescence and/or ISC as competing decay processes, leading to an increase in ^{3}DOM* and $^1O_2$ quantum yields (Φ_{1O2}) and/or an increase in Φ_f.

It has been demonstrated that ozone treatment results in changes of the properties of DOM.[30] This includes a decrease in absorbance and fluorescence intensity, reduction in electron donating capacity and in the hydrophobicity of the DOM, formation of easily biodegradable low molecular weight compounds such as aldehydes, ketones carboxylic acids, and decrease in the chemical oxygen demand.[30-36] It was observed that ozonation of phenols, commonly found in DOM and highly reactive towards ozone, resulted in the formation of quinones, catechols and muconic acid, while the ozonation of olefins produced hydrogen peroxide, aldehydes, ketones, hydroperoxides and carboxylic acids.[30, 37-40]

When considering the interaction between engineered and natural systems, there is a need to consider the effect that unit treatment operations can have on the subsequent chemistry in a natural system receiving the treated water. For example, there is significant interest in the use of additional polishing steps following conventional wastewater treatment to disinfect water discharged to bathing streams or lakes and to water resources and to remove micropollutants.[41-44] In these cases, the effect of engineered systems, for example the application of oxidants such as ozone, on the photochemical properties of DOM need to be considered. In a previous study, Mostafa and Rosario-Ortiz evaluated the effect of ozone on the formation of $^1O_2$ from DOM and wastewater-derived effluent organic matter (EfOM). The application of ozone resulted in an increase in the quantum yield for $^1O_2$ formation (Φ_{1O2}).[45]

The objective of this study was to evaluate the effects of ozone treatment on the photophysical and photochemical properties of DOM. Ozonated samples were characterized via absorbance and fluorescence spectroscopy and the Φ_{1O2} and Φ_f were determined. As the distribution of products and the rate constants of ozone reactions are pH-dependent for moieties such as phenols and amines, [30] the experiments were conducted at pH 3 and 7 to help differentiate

between the contributions of these moieties. The relationships between the changes in fluorescence and the formation of $^1O_2$ were also evaluated, to acquire a better understanding of the fundamental photophysical and photochemical processes happening with DOM.

Materials and Methods

Chemicals and solutions

All chemicals were commercially available and used as received, except for *p*-nitroanisole, which was recrystallized from ethanol prior to utilization. A complete list of the chemicals is provided in the SI, Text S1. All solutions were prepared in ultrapure water (resistivity 18.2 MΩ cm) obtained from a Sartorios Stedim dispenser. 100 mM Phosphate buffer stock solutions were prepared by mixing sodium phosphate salts and phosphoric acid solutions to the desired pH.

Two DOM isolates from the International Humic Substances Society (St. Paul, Minnesota) were selected as representatives of autochthonous (Pony Lake fulvic acid (PLFA), 1R109F) and allochthonous (Suwannee River fulvic acid (SRFA), 1S101F) samples. The carbon content of the DOM stock solutions was measured by spectrophotometry using the specific ultraviolet absorbance values at the wavelength λ = 254nm ($SUVA_{254}$) (4.2 and 2.5 L mg_C^{-1} m^{-1} for SRFA and PLFA, respectively).[31] DOM stock solutions ≈ 50 mg_C L^{-1} in 10 mM pH 7.0 phosphate buffer were prepared. After 2 – 4 hours of stirring, the solutions were filtered with ultrapure water prewashed 0.45 μm polyethersulfone filters (Whatman). Experiments were carried out at pH 3 and pH 7 in 10 mM phosphate buffer. A surface water sample was collected from the San Juan River (SJR) near Farmington, New Mexico. The DOC was 3.65 mg_C L^{-1} as measured by a TOC analyzer (see below) and the alkalinity 115 mg L^{-1} as $CaCO_3$. The SJR water was used unbuffered and it should be noted that for the SJR experiments, the samples were diluted because of the addition of the ozone stock solution. To allow for a better mutual comparison between samples, the same dilution factor (50%) was used in all SJR experiments by adding the appropriate amount of ultrapure water.

Analytical instrumentation

UV-Vis spectra were measured on a Cary 100 Bio UV-Visible spectrophotometer using 1, 5 or 10 cm path length quartz cuvettes. The pH was measured using a calibrated Orion Star A211 pH-meter using a Thermo Scientific Orion pH electrode model 8157BNUMD. DOC was measured on a Sievers TOC analyzer model M5310C.

Concentrations of the probe compounds and of the actinometer were measured in duplicate on an Agilent 1200 series high-performance liquid chromatography (HPLC) system equipped with an Agilent Eclipse Plus C-18 5 μm particle size reverse-phase column, a UV-Vis absorbance and a fluorescence detector using the isocratic methods detailed in the SI, Table S1. Fluorescence spectra were measured at room temperature (21 ± 1 °C) using a Horiba Scientific FluoroMax-4 spectrofluorometer.

Measurement of optical parameters

Fluorescence spectra were measured at excitation wavelengths (λ_{ex}) ranging from 240 to 550 nm in 10 nm increments, with emission intensity collected from 300 to 700 nm in 2 nm increments. An integration time of 0.25 s and bandpass of 5 nm were used. Spectra were collected in signal divided by reference mode and were processed using previously published methods,[46, 47] which included applying instrument-specific correction factors, blank subtraction, excising Rayleigh scatter, inner filter corrections, and Raman normalization. Values for Φ_f were calculated using previously described methods with a few exceptions that are described in the SI, Text S4. [47, 48]

The UV-Vis absorbance spectra were used to calculate additional optical/physicochemical parameters. The ratio of the absorbance at λ = 250 nm over the absorbance at λ = 365 nm is defined as the *E2/E3* ratio. The $SUVA_{254}$ (unit L mg_C^{-1} m^{-1}) of the DOM solutions was calculated by

dividing the absorbance by the optical path length and carbon concentration.[49] The spectral slope (*S*),[50] which is the exponential coefficient obtained from a single-exponential fit to the absorbance spectra (*Abs*) in the range of 300-600 nm, was calculated according to eq. 4 using a one-parameter fit (*S*) and $Abs_{\lambda=350nm}$ as constant. The wavelength-averaged specific absorption coefficient ($SUVA_{avg}$, units of L mg_C^{-1} m^{-1}), which is a proxy for the amount of light absorbed by the sample in the interval 290-400nm, was calculated by integrating the product of the specific absorption coefficients ($SUVA_\lambda$) and the spectral photon irradiance of the solar simulator (I_λ, units of E m^{-2} nm^{-1} s^{-1}) over the selected wavelength range and normalizing over the integral photon irradiance (see below, eq. 5).

$$Abs_\lambda = Abs_{\lambda=350nm} e^{-S(\lambda-350\text{nm})} \quad (4)$$

$$SUVA_{\text{avg}} = \frac{\int_{290\text{ nm}}^{400\text{ nm}} SUVA_\lambda I_\lambda d\lambda}{\int_{290\text{ nm}}^{400\text{ nm}} I_\lambda d\lambda} \quad (5)$$

Ozonation experiments

An ozone/oxygen gas mixture was obtained from an Ozone Solutions ozone generator model TG-40 and bubbled in a 2°C water-jacketed 2L glass vessel filled with ultrapure water. The obtained ozone stock solution had a concentration of ≈ 45 mgO_3 L^{-1} and was spiked into the DOM-containing solutions at various specific ozone doses (≤ 1 $mmol_{O3}$ $mmol_C^{-1}$), similar to ozonation steps in a drinking or wastewater treatment (0.36-1.16 mgO_3 mg_C^{-1} [41]). After ozonation, the solutions were kept closed for a minimum of two days under refrigerated condition (4°C) to allow complete ozone consumption. The exact ozone concentration in the stock solution was measured spectrophotometrically using a 2mm pathlength quartz cuvette and an absorption coefficient of

189 3200 $M^{-1}cm^{-1}$ at 260nm.[30] The DOC concentration after ozone addition was 5mg_C L^{-1} for PLFA
190 and SRFA and 1.8mg_C L^{-1} for the SJR water. For all the experiments but one of the SJR experiment
191 series, 0.1 M *t*-butanol was added as an •OH radical quencher. The presence of *t*-butanol does not
192 affect the DOM fluorescence or the $^1O_2$ and ^{3}DOM* measurements. [36]

193 **Irradiation experiments**

194 To measure the production of $^1O_2$ and ^{3}DOM*, irradiation experiments were conducted at
195 least in duplicate using an Oriel Sol1A solar simulator equipped with a 1000W xenon lamp. The
196 spectral distribution of the lamp was measured using a calibrated Ocean Optics USB2000
197 spectrometer (see Figure S1 (SI) for a spectrum of the photon irradiance of the simulator).
198 Ozonated DOM solutions spiked with probe compounds were irradiated in 5 mL glass vials
199 (absorbance and transmittance spectra given in the SI, Figure S2) lying at an angle of $\approx 30^\circ$ degrees
200 from the horizontal. Samples were temperature-controlled at 20 $\pm 1^\circ$ C using a recirculating chiller.
201 Solution aliquots were taken at regular time intervals and the concentrations of the probe
202 compounds were analyzed in duplicate using the aforementioned HPLC methods.

203 The methods to determine the $[^1O_2]_{ss}$, Φ_{1O2} and of ^{3}DOM* reactivity using probe
204 compounds are described elsewhere[5] (see also SI, Texts S2 and S3). Briefly, the $[^1O_2]_{ss}$ and Φ_{1O2}
205 were measured by 22.5 μM furfuryl alcohol (FFA) as a probe compound and ^{3}DOM* reactivity
206 was determined by using 10 μM 2,4,6-trimethylphenol (TMP) or 10 μM 3,4-dimethoxyphenol
207 (DMOP) and reported as f_{TMP} and f_{DMOP}, the quantum efficiency for the disappearance of the
208 ^{3}DOM* probe compound (the pseudo-first-order phototransformation rate constant of the probe
209 divided by the rate of light absorption, SI, Text S3). Pseudo-first-order depletion rate constants
210 were determined by non-linear fitting to a first-order kinetic rate constant equation using the
211 software OriginPro 2017.

The daily photon irradiance of the simulator was determined by a *p*-nitroanisole (PNA)/pyridine actinometer using a concentration of 10 μM of PNA and 5 mM of pyridine. At this pyridine concentration the PNA quantum yield is 1.74×10^{-3}.[51] To compensate for the variation of the xenon lamp intensity between experiments, all results were normalized by using the daily measured PNA depletion rate constant to the average PNA depletion rate constants (2.09×10^{-4} s^{-1}). The photon fluence rate in the interval λ = 290 – 400 nm was calculated to be of 5.61×10^{-4} einstein m^{-2} s^{-1} using eq. S3.

Results and discussion

Effects of ozonation on the optical properties of the DOM

Rationale of the ozonation experiments

Ozone is a selective oxidant that reacts preferentially with phenols, which are an important fraction of the pool of DOM chromophores.[36] In a recent studies the reactions between ozone and DOM and model phenols, were examined in detail.[52] The reactions of ozone with phenols are characterized by high second-order rate constants [40, 53, 54] and a pH dependent product distribution, quinones representing one of the main classes of products.[39] As the reactivity pK_a (i.e., the pH at which half of the reactivity is due to phenol or phenolate, respectively) of phenols toward ozone is ≈4, [30] we performed ozone treatments at pH 3 and pH 7, because at these pH values the reactivity is dominated by phenol or phenolate, respectively. Additional information on the reaction of ozone with phenols are given in the SI, Text S6.

Absorption properties

Prior to the application of ozone, PLFA and SRFA had wavelength-averaged specific absorption coefficient ($SUVA_{avg}$, see eq. 5) values of 0.65 and 1.5 L $mg_C^{-1}m^{-1}$ at pH 7 and 0.45 and 0.88 L $mg_C^{-1}m^{-1}$ at pH 3, respectively (see Figure S3, SI). SRFA is an allochthonous DOM (originated from the degradation of plants) and its higher specific absorption coefficients compared to PLFA (an autochthonous DOM mostly originating from bacteria and algae) reflects its stronger aromatic character. The differences in light absorption between the two pH values reflect the speciation of the carboxylic groups in the DOM. Ozonation induced a marked decrease in $SUVA_{avg}$ for both DOM samples at each pH examined (Figure 1). Most of the decrease is observed at low specific ozone doses (0 to 0.2 $mmol_{O3}$ $mmol_C^{-1}$) and further ozonation reduces the $SUVA_{avg}$ only moderately (Figure S4, SI). Using the $SUVA_{avg}$ as a proxy for the amount of light absorbed by the samples, it can be observed that for the two types of DOM and at the two investigated pH values, the $SUVA_{avg}$ decreases by a factor of 4.1 – 5.9 for a specific ozone dose of 0.25 $mmol_{O3}$ $mmol_C^{-1}$ applied to untreated samples, but only by a factor 1.2 – 2.1 for successive applications of the same specific ozone dose of 0.25 $mmol_{O3}$ $mmol_C^{-1}$ (for detailed data see the SI, Table S2). The $SUVA_{avg}$ values are higher at pH 7 than at pH 3 for the low specific ozone doses, a behavior that changes for the high doses ($\geq$ 0.5 $mmol_{O3}$ $mmol_C^{-1}$) where the $SUVA_{avg}$ values are more important for the pH 3 experiments.

The absolute decrease in absorption is more important at shorter wavelength but the relative decrease is more marked at longer wavelengths as it can be seen using the ratio $A_{O3}/A_{O3=0}$. (Figures 1 and S5, SI). A marked difference in this can be observed for SRFA for different pHs, with a more important decrease at long wavelengths (λ > 350 nm) for pH 3 than for pH 7 (see SI, Table

S2). For PLFA the difference in the ratio between the two pH values is relatively limited. It should also be noted that the difference in absorption at pH 3 and pH 7 decreases with increasing specific ozone doses.

The stronger relative decrease in absorbance at longer wavelength (λ > 350 nm) is probably due to a more efficient removal of chromophores absorbing at these wavelengths. These chromophores are expected to be relatively large conjugated electronic systems having a high ozone reactivity and prone to lead to ring opening products that do not absorb light at these longer wavelengths. At shorter wavelengths, the smaller relative decrease in absorbance might result from a reduced removal of more ozone-resistant chromophores as well as an additional absorption due to ozonation products, such as quinones.

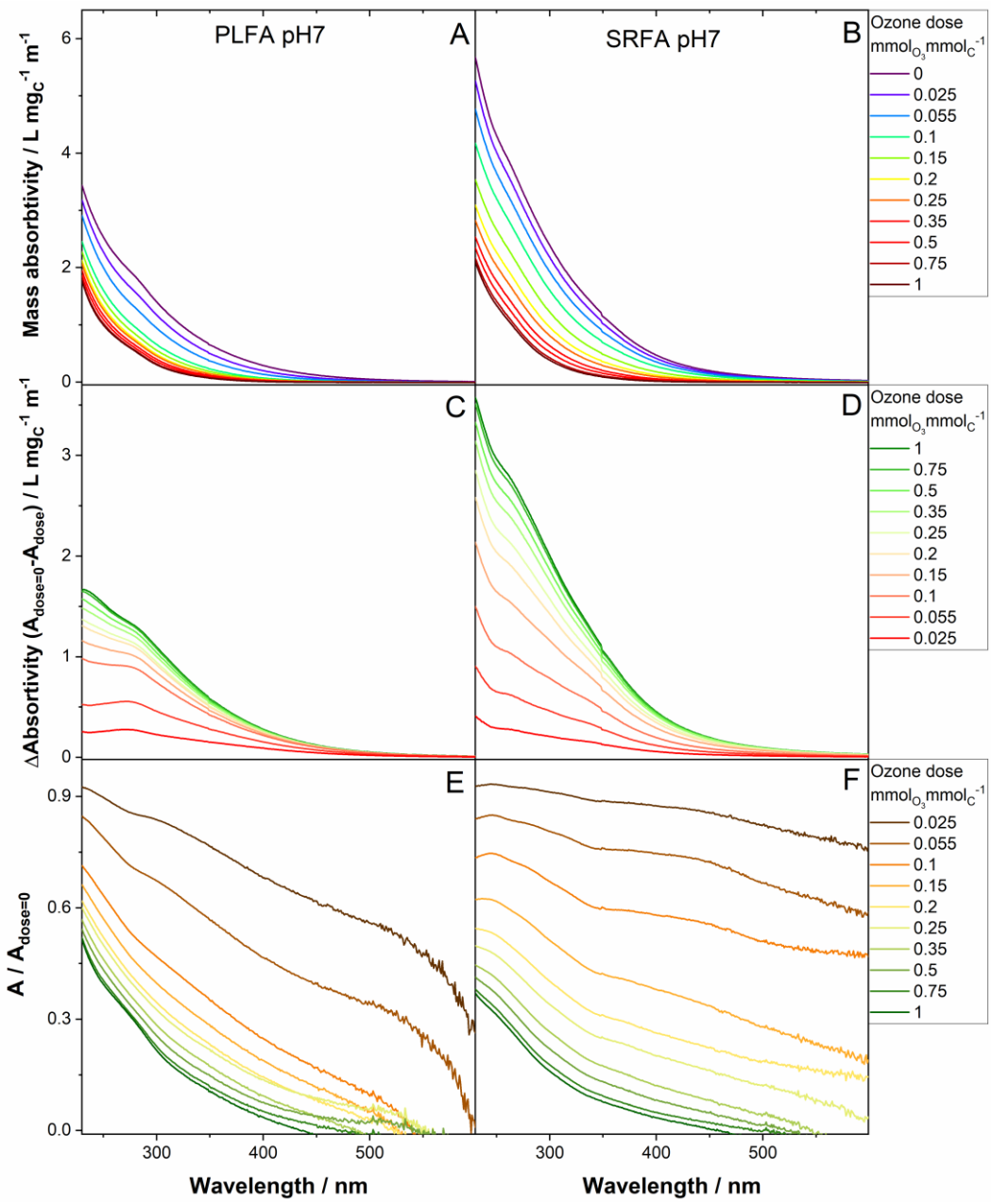

Figure 1. Effects of ozone on the absorbance of the two DOM samples at pH 7 (10 mM phosphate buffer). A and B: mass absorptivity as a function of the specific ozone doses for Pony Lake fulvic acid (PLFA, panel A) and Suwannee River fulvic acid (SRFA, panel B). C and D: Variation of the absorptivity ($A-A_{O3=0}$) for PLFA and SRFA respectively. E and F: Ratio of the absorptivity (A_{O3} / $A_{O3=0}$) for PLFA and SRFA respectively, data for wavelength $\lambda>500$ nm are noisier due to the low absorbance of the solutions. Ozonation experiments were performed in the presence of 0.1M *t*-butanol as a hydroxyl radical scavenger. Figure S5, SI presents the same data set for pH 3.

Fluorescence properties

Figure 2A shows the fluorescence intensity as a function of the specific ozone dose for the excitation wavelength λ = 370 nm, a wavelength chosen due to instrumental limitations (see SI, Text S4). Figure 2A shows that as the specific ozone doses increase, the fluorescence intensity undergoes an exponential-like decrease. The $SUVA_{370}$ behaves similarly with an exponential-like decrease as a function of the ozone dose (Figure 2B), but the relative decrease in $SUVA_{370}$ is more important than the relative decrease in fluorescence intensity. From this comparison it can be concluded that Φ_f (i.e., the fluorescence intensity over the amount of light absorbed, see also eq. 1) at the wavelength 370 nm is increasing, as has been reported previously.[36]

Φ_f does not increase proportionally to the specific ozone dose (Figure 2C). For PLFA, Φ_f increases strongly for specific ozone doses of 0 – 0.2 $mmol_{O3}$ $mmol_C^{-1}$, but remains almost constant at ≈3 % for higher specific ozone doses. The observed behavior for PLFA is independent of pH (Figure 2C). In contrast, for SRFA there is a clear pH effect. At pH 3, there is a less pronounced increase compared to PLFA, reaching a plateau at a similar specific ozone dose of 0.2 $mmol_{O3}$ $mmol_C^{-1}$. However, at pH 7, there seems to be a linear increase in Φ_f for specific ozone doses of < 0.5 $mmol_{O3}$ $mmol_C^{-1}$, followed by a slower increase beyond this point. A similar behavior was observed in a previous study.[36]

Similar to the explanation of absorbance changes, it can be postulated that multiple groups of fluorophores react with ozone at different rates. At low specific ozone doses, one class of fluorophores reacts rapidly. However, at higher ozone doses there is no significant change in Φ_f, indicating that there is a pool of fluorophores which is relatively recalcitrant to ozonation. The mechanistic interpretations presented later in the manuscript (see section *Mechanistic interpretations*) indicate that the fluorophores with low Φ_f are selectively removed by ozonation.

297

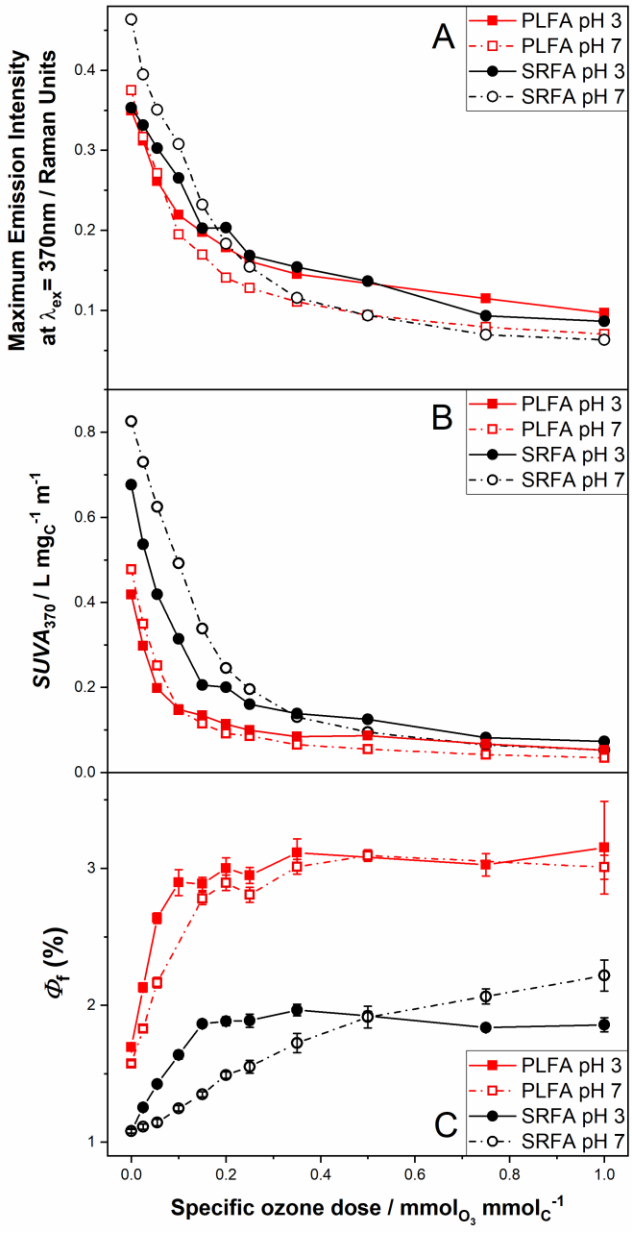

298

299 **Figure 2.** Effect of ozonation (specific ozone dose) of SRFA and PLFA at pH 3 and 7 on the
300 fluorescence intensities, $SUVA_{370}$ and quantum yields. (A) Maximum fluorescence emission
301 intensity at the excitation wavelength λ = 370 nm. The maximum emission wavelengths at this
302 excitation wavelength varied between 444 and 476 nm. (B) Specific UV absorbance at the
303 wavelength λ = 370 nm ($SUVA_{370}$). (C) Maximum quantum yield (Φ_f). Solutions were buffered
304 by 10 mM phosphate buffer. Error bars represent the standard errors from the mean of triplicate
305 fluorescence measurements. Measurements were conducted in duplicate or triplicate
306 (fluorescence). Ozonation experiments were performed in the presence of 0.1 M *t*-butanol as a
307 hydroxyl radical scavenger.

Effects of ozonation on the photogeneration of transient species

Singlet oxygen ($^1O_2$)

The formation of $^1O_2$ was evaluated during simulated sunlight irradiation for DOM containing samples treated with increasing specific ozone doses. Figure 3A presents the steady state concentration of $^1O_2$ ($[^1O_2]_{ss}$) measured after pre-treatment of the samples with various specific ozone doses. Without ozonation, $[^1O_2]_{ss}$ values were in the range of $2.1 - 2.5 \times 10^{-13}$ M and similar for the two examined pHs. At very low specific ozone doses (<0.05 $mmolO_3$ $mmolC^{-1}$) an increase in $[^1O_2]_{ss}$ can be observed (significant for all samples but PLFA at pH 7). The observed increase in $[^1O_2]_{ss}$ for the very low ozone doses should be attributed to the aforementioned conversion of phenol to quinones moieties upon ozonation (SI, text S6), quinones having generally a higher potential to generate $^1O_2$ than phenols.[55] For higher specific ozone doses, $[^1O_2]_{ss}$ values decreased by a factor ≈2. Given that the $SUVA_{avg}$ of the samples decreased by a factor 10 – 20 (Figure S3, SI), a more pronounced decrease of the $[^1O_2]_{ss}$ was expected.

Figure 3B shows that the Φ_{1O2} increased as a function of ozone dose. This is in agreement with a previous observation [45] and is confirmed in this study with a better resolution of the specific ozone doses. The $^1O_2$ formation also depended on the pH and the sample type. PLFA had the highest Φ_{1O2} and resulted in a larger increase, towards values of more than 16% for a specific ozone dose of 1 $mmol_{O3}$ $mmol_C^{-1}$. For SRFA, the extent of the increase was lower, reaching values of ≤ 13% for high specific ozone doses (≥ 0.5$mmol_{O3}$ $mmol_C^{-1}$), however, the relative increase in Φ_{1O2} is similar for both fulvic acids. The observed Φ_{1O2} values at pH 3 are usually higher than at pH 7 for the low ozone doses and lower for the high ozone doses, which could be related to the

distribution of products from the phenolic groups toward ozone being pH dependent (see SI, text S6). [52]

There is significant data available on Φ_{1O2} values for DOM and typically a range of 0.5 to 5.5 % was found.[15-22] In all cases, the previously reported values are clustered in a lower range than observed in this study for ozonated samples. Interestingly, Φ_{1O2} values of up to 12% have been reported for fog waters collected in Davis, CA and Baton Rouge, LA, USA.[56] As ozone is an important atmospheric oxidant involved in the formation and aging of atmospheric organic aerosol,[57] it can be hypothesized that the structures produced upon ozone-induced transformation of atmospheric organic matter and aquatic organic matter are similar.

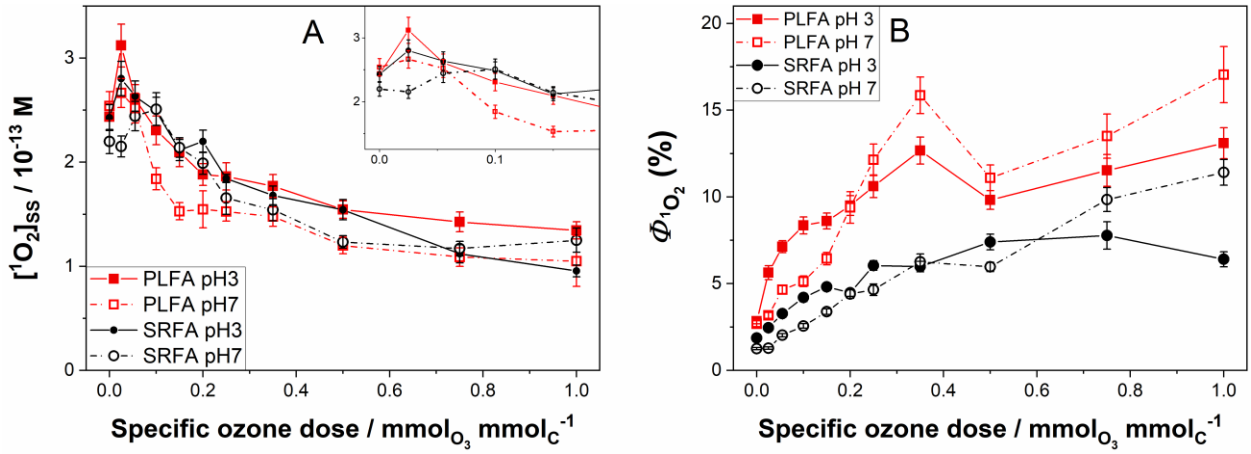

Figure 3. Singlet oxygen steady-state concentrations and singlet oxygen quantum yields for PLFA and SRFA samples (5mg$_C$ L^{-1}) under simulated sunlight irradiation (290-400 nm) without and with ozone pre-treatment (variation of specific ozone doses). (A) Measured singlet oxygen ($^1O_2$) steady-state concentrations. Inset, enlarged view for low specific ozone doses. (B) Singlet oxygen quantum yields (Φ_{1O2}). Red symbols/lines: PLFA; black symbols/lines: SRFA. pH 3: full symbols; pH 7: open symbols. Solutions were buffered with 10 mM phosphate buffer at either pH value. Error bars represent standard errors obtained from the pseudo-first order fittings (FFA experiments in duplicate). Ozonation experiments were performed in the presence of 0.1 M *t*-butanol as a hydroxyl radical scavenger.

Correlations between DOM optical properties and the reactive intermediate generation potential

Changes in various DOM optical properties as a function of the specific ozone dose are presented in Figure S6. There is a decrease in the $SUVA_{254}$ and an increase in both the *E2/E3* ratio and spectral slope with increasing specific ozone doses. These trends are consistent with previous reports on the effect of ozone on DOM optical properties.[31, 45] Each of these optical properties has been correlated to DOM molecular weight and aromaticity. [49, 58, 59] There are relatively good linear correlations between $\Phi_{^1O_2}$ and *E2/E3* or the spectral slope *S* (Figures 4A and S7A and B, SI), which has been observed previously for non-ozonated isolates as well as whole water samples of varying DOM sources and character.[27] Ozone reacts mainly with activated aromatic moieties in DOM, wherefore, the observed effects on optical properties are likely the result of a decreasing aromatic carbon content. The observed regression coefficient for the *E2/E3* value vs $\Phi_{^1O_2}$ from a previous study and from this study are very similar (Table S4, SI), indicating that *E2/E3* is a good predictor of $\Phi_{^1O_2}$. Similarly to $\Phi_{^1O_2}$, there is also a good linear correlations between f_{TMP} or f_{DMOP} and *E2/E3*, *S*, and $SUVA_{254}$ (Figures S7D – S7I, SI), this should be related to the ratio [^{3}DOM*] / [$^1O_2$] being constant (see SI, text S9).

A moderate decrease (≈30%) of the phototransformation rate constants of the ^{3}DOM* probe compound TMP as a function of the specific ozone dose is observed for PLFA while more or less stable rate constants are observed for SRFA (see SI, Figure S10). As the ratio [^{3}DOM*] / [$^1O_2$] was determined to be constant for both fulvic acids (see SI, Text S9), the observed TMP behavior can be attributed, similarly as discussed above for $\Phi_{^1O_2}$, to an increase in ^{3}DOM* production quantum yield. These results are in stark contrast with observations in Ref. 32, where an important decrease (≈80%) in the phototransformation rate constant of TMP as a function of

372 the specific ozone dose is observed for the same PLFA and SRFA. These two apparently
373 contradictory observations can be attributed to the differences in irradiation conditions between
374 the two studies. The filtered light from the medium pressure Hg lamp used in Ref. 32 is mainly
375 absorbed by DOM at the wavelength λ = 366 nm (with only a minor contribution at λ = 334), while
376 the main absorption by DOM of the simulated sunlight used in this study occurs at shorter
377 wavelengths. As the decrease in UV-Vis absorbance is more important at longer wavelengths (see
378 Figure 1), the amount of light absorbed under medium pressure Hg lamp irradiation decreases
379 faster with increasing ozone dose (e.g., for SRFA at the specific ozone dose of 0.5 $mmol_{O3}$ $mmol_{C}^{-1}$
380 ^{1}, the relative decrease in light absorption is 5 times more important in the Ref. 32 setup compared
381 to our study, see the SI, Table S3) compared to simulated sunlight irradiation.

382 Figure 4B presents Φ_f as a function of *E2/E3* for the two DOM isolates treated using
383 variable specific ozone doses. A linear relationship between the two quantities can be observed for
384 low *E2/E3* values (<15). However, for higher *E2/E3* values the Φ_f levels off except for SRFA at
385 pH 7 where the same relationship is observed for the full range of *E2/E3* values. Figure 4C presents
386 Φ_{1O2} vs Φ_f as a function of the ozone dose. For low Φ_{1O2} values a linear correlation between the
387 two quantum yields can be observed, but for higher Φ_{1O2} values Φ_f levels off. This result can be
388 rationalized by assuming that the pool of chromophores in the DOM that determines its
389 fluorescence is different from the pool of chromophores responsible for the generation of $^{1}O_2$.
390 Quinone and ketone moieties of the DOM are expected to dominate the generation of $^{1}O_2$ under
391 irradiation, while the variety of chromophores responsible for the fluorescence of DOM is
392 probably much broader.

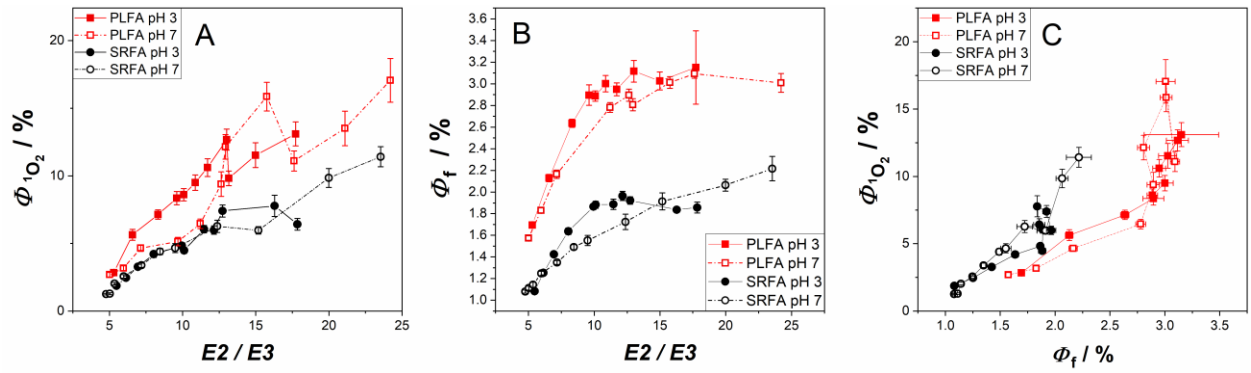

Figure 4. Relationship between quantum yields and optical parameters. (A) Singlet oxygen production quantum yield (Φ_{1O2}) as a function of the *E2/E3* absorbance ratio. (B) Fluorescence quantum yield (Φ_f) as a function of the *E2/E3* absorbance ratio. (C) Φ_{1O2} vs Φ_f. Red symbols/lines: PLFA; black symbols/lines: SRFA. pH 3: full symbols; pH 7: open symbols. Solutions were buffered with 10 mM phosphate buffer. Error bars represent standard errors obtained from the pseudo-first-order fittings (FFA experiments, in duplicate) for $^1O_2$ and from the mean of triplicate measurements (fluorescence). Ozonation experiments were performed in the presence of 0.1 M *t*-butanol as a hydroxyl radical scavenger.

Mechanistic interpretations

The obtained results suggest that both the Φ_f and the Φ_{1O2} increase with increasing specific ozone doses applied to the DOM-containing samples (Figure 4C). A similar trend has also been observed for $^{\bullet}OH$ formation rate vs the fluorescence intensity.[26] We postulate that ozonation induces a decrease of the internal conversion rate, $k^{IC}_{^1DOM^*}$, leading to an increase in Φ_f.

The main factor that influences $k^{IC}_{^1DOM^*}$ (SI, eq. S13) is the energy needed for the electronic transition from the first-excited singlet state (S_1) to the ground electronic state (S_0), $k^{IC}_{^1DOM^*}$ being inversely proportional to the $S_1 \rightarrow S_0$ energy gap. [60, 61] $k^{IC}_{^1DOM^*}$ can be estimated using the energy gap law (eq. 6), where $\Delta E_{S1\rightarrow S0}$ is the energy of the $S_1 \rightarrow S_0$ transition in J mol^{-1} and α a proportionality constant. [60]

$$k^{IC}_{^1DOM^*} / s^{-1} \approx 10^{13} \exp(-\alpha\, \Delta E_{S1\rightarrow S0}) \quad (6)$$

A classical method to determine $\Delta E_{S1\rightarrow S0}$ for fluorescent molecules is to use the mirror image rule (the fluorescent spectra is the mirror image of the $S_0 \rightarrow S_1$ absorbance spectra) plotting both spectra on the same figure, $\Delta E_{S1\rightarrow S0}$ is equal to the energy at the intersection of the two spectra. [61] For DOM, being a mixture of molecules, this method cannot be used. We postulate here that for DOM, the variation of the mean energy of the $S_1 \rightarrow S_0$ transition can be estimated by measuring the variation of the wavelength of maximum fluorescence emission ($\lambda_{F,max}$). Indeed, fluorescence occurs from the S_1 to the S_0 electronic state (Kasha's rule) and for the chromophore vibrational levels it occurs from the lowest vibrational level of the S_1 state to one of the lower vibrational levels of the S_0 state.[62] It is reasonable to assume that the receiving vibrational level is not shifting significantly with ozonation, in which case, $\lambda_{F,max}$ corresponds to the energy of the $S_1 \rightarrow S_0$ transition ($\Delta E_{S1\rightarrow S0}$) plus a constant term that corresponds to the mean vibrational level of the receiving S_0 state (see SI eq. S24).

Figure S10 presents $\lambda_{F,max}$ vs the specific ozone dose with the corresponding photon energy as a right axis. An increase in photon energy with an increasing extent of ozonation is observed, with most of the increase already observed for low specific ozone doses (≤ 0.2 $mmol_{O3}$ $mmol_C^{-1}$). This indicates that the mean energy of the $S_1 \rightarrow S_0$ transition is increasing during ozonation, inducing a decrease in the non-radiative decay rate and a relative increase in Φ_f. Application of the energy gap law (eq. 6, see Text S8 and Table S6) indicates that the observed increase in Φ_f is due to an increase in the mean $\Delta E_{S1\rightarrow S0}$ that induces a decrease in $k^{IC}_{^1DOM^*}$ and applying eq. S23 to an increase in Φ_f. This implies that ozonation is selectively removing chromophores with a low ($\Delta E_{S1\rightarrow S0}$) and low Φ_f. This selective removal can be attributed to the fact that chromophores that absorb well into the visible ($\lambda > 500$ nm) have large conjugated systems with low $S_1 \rightarrow S_0$ energy

436 gaps. These chromophores are expected to be electron rich and, therefore, highly susceptible to
437 oxidation by ozone.

438 The application of the energy gap law would also predict an increase in Φ_{1O2} similar to the
439 one observed for $\Phi_{f.}$. This is insufficient to explain the observed increase in Φ_{1O2}. One possibility
440 that was evaluated regarding the increase in Φ_{1O2} was whether ozone impacted the intersystem
441 crossing in DOM, yielding a higher concentration of ^{3}DOM*. Text S9 in the SI describes our
442 results. Ultimately, we attribute the observed Φ_{1O2} increase to the formation of quinone-like
443 moieties from the ozonation of phenols. Quinones and aromatic ketones, having generally
444 important intersystem crossing rates, are believed to be the main DOM chromophores precursors
445 of ^{3}DOM* under irradiation. [55]

446 It is still worth noting that other effects could also be at play, given the complexity of DOM.
447 For example, it is plausible that the observed relationship between Φ_f and Φ_{1O2} are purely
448 fortuitous and the result of independent processes where different pools of fluorophores and singlet
449 oxygen sensitizers are reacting with ozone and resulting in the removal of the ozone reactive
450 components. This could also yield the observed result if the less reactive groups towards
451 fluorescence and singlet oxygen formation were equally highly reactive with ozone.

452

453 **Effects of ozonation on the optical properties and the $^1O_2$ generation potential of a natural**
454 **water with and without a hydroxyl radical ($^{\bullet}$OH) scavenger**

455 Ozonation was performed with SJR water in the absence and in the presence of a $^{\bullet}$OH
456 scavenger (Figures 5 and S8, SI). In the presence of a $^{\bullet}$OH scavenger, the observed results are
457 comparable to the two DOM isolates, with a decrease in absorbance and an important increase in

458 Φ_{1O2} (from 4.9 to 8.8 %) for specific ozone doses ≤ 0.2 $mmol_{O3}$ $mmol_C^{-1}$. In the absence of a •OH
459 scavenger, a much more important decrease in the light absorbance properties and a relatively
460 smaller increase in Φ_{1O2} is observed. If ozonation of DOM induces a large increase in Φ_{1O2}, such
461 an effect should not necessarily be expected of the •OH-induced oxidation.

462 In the absence of an •OH scavenger, the •OH radicals produced during reaction between
463 DOM and ozone have two effects: (1) to catalyze ozone decomposition, yielding a lower overall
464 ozone exposure, (2) reaction of both •OH and O_3 with DOM moieties.[30, 63] A previous study showed
465 that for a humic acid the first effect was dominant and that •OH induced a smaller bleaching of the
466 humic acid (as seen as a smaller reduction of the $SUVA_{254}$ upon ozonation in the absence of a •OH
467 scavenger), while for PLFA and SRFA the second effect was dominating and the presence of •OH
468 produced a more important bleaching of the DOM, [31] similarly as what is observed here for the
469 SJR water.

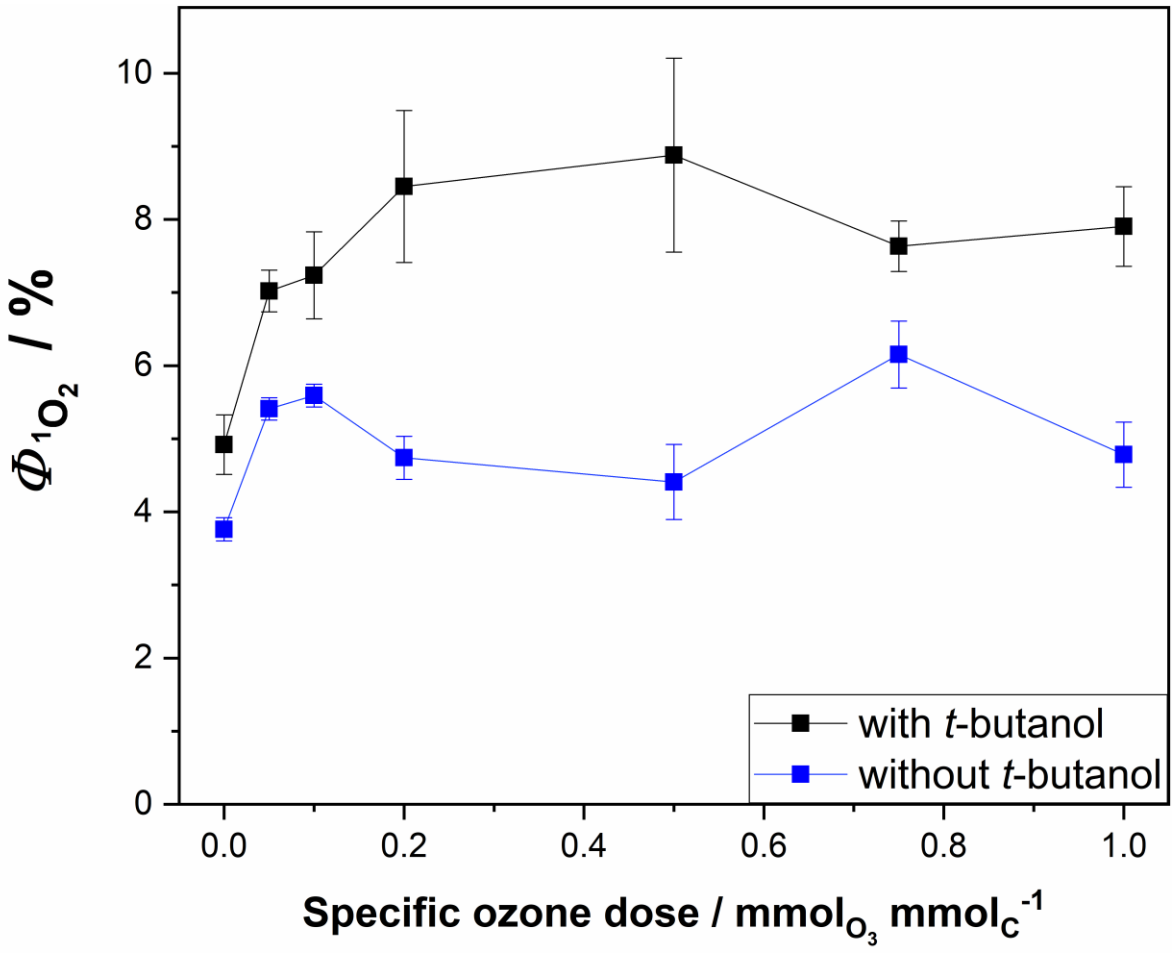

Figure 5. Singlet oxygen quantum yield as a function of the specific ozone dose for the San Juan River (SJR) water, ozonation experiments conducted in the absence (blue) and in the presence (black) of 0.1M *t*-butanol as a hydroxyl radical scavenger.

Environmental implications

Ozonation is increasingly used as a polishing step in wastewater treatment to abate micropollutants.[41, 42] Ozone will have the effects to decrease the light absorbance of the wastewater DOM at all wavelengths and if the wastewater is a significant fraction of the receiving water body leading to an overall improved perception of the water to be more pristine. A decrease in light absorbance by DOM leads to an increase in water transparency and consequently in transformation

rates of micropollutants due to direct photolysis and nitrate-induced indirect phototransformation through the produced hydroxyl radical. The effect of ozone treatment on the production of ^{3}DOM* and $^1O_2$ in the top water layer includes an enhancing component due to the aforementioned increased water transparency, a decreasing component due to a reduced rate of light absorption, as well as an additional enhancing component due to the increase in ^{3}DOM* and $^1O_2$ formation quantum yields. Considering deeper water bodies, where all photochemically active sunlight is absorbed, the overall production and concentration of ^{3}DOM* and $^1O_2$ will increase due to the increased quantum yields of their formation.

The aforementioned qualitative trends were verified using photochemical modeling with simple scenarios. Briefly, for the modeling a solar spectrum at air mass 1.5 and a 1 m light path length were employed. In a first scenario, 5 $mg_C\ L^{-1}$ of PLFA treated with a 1 $mmolO_3\ mmol_C^{-1}$ ozone dose at pH 7 was considered as DOM, and an optically thin concentration of nitrate ($\leq$1 $mgNO_3^-\ L^{-1}$) was employed. Details of the modeling and calculations are given in the SI, Text S7. Under such conditions, ozonation of PLFA induces an increase in $^{\bullet}$OH production from nitrate photolysis by 54% and a decrease of $^1O_2$ production by 18% (see Figure 6, panels B and C). As wastewater rarely represent 100% of the water in a receiving body, a second scenario with 80 w/w % of untreated water (PLFA, O_3 =0 $mmolO_3\ mmol_C^{-1}$) and 20% of ozonated water (PLFA, O_3 =1 $mmolO_3\ mmol_C^{-1}$) was considered. In this case, the $^{\bullet}$OH production rate from nitrate photolysis increases by 8% and the $^1O_2$ production decreases by 5% (compared to the non-ozonated PLFA). 98% of the light in the interval 290 – 400 nm is absorbed by the non-treated fraction of the water in this scenario, while the treated fraction would only absorb the remaining 2% of the light. It should be noted that ozonation would importantly affect the phototransformation of micropollutants only in the cases in which the treated wastewater represents an important

absorbance fraction of the whole water, e.g., when wastewater is discharged in a pristine low DOM surface water body.

Model calculations were also performed to assess changes in direct and indirect photolysis rates of two selected micropollutants. The antibiotic ormetoprim, a compound that is mostly subject to indirect photolysis, and the sunscreen agent 4-aminobenzoic acid, a compound that is mostly affected by direct photolysis, were chosen because kinetic data on their photolysis is available.[64] It should be noted than the effects of •OH on the phototransformation of the two micropollutants were not calculated in this scenario as •OH was seen to not be an important factor in the phototransformation of these two compounds. [64] For the scenario with total ozonation of the water, a reduction of the phototransformation rate of ormetoprim by 7% and an increase in phototransformation of 4-aminobenzoic acid by 35% are predicted. For the 80/20 w/w % mix scenario, the phototransformation rate of ormetoprim is predicted to decrease by 3% while it is predicted to increase by 5% for 4-aminobenzoic acid (see Figure 6).

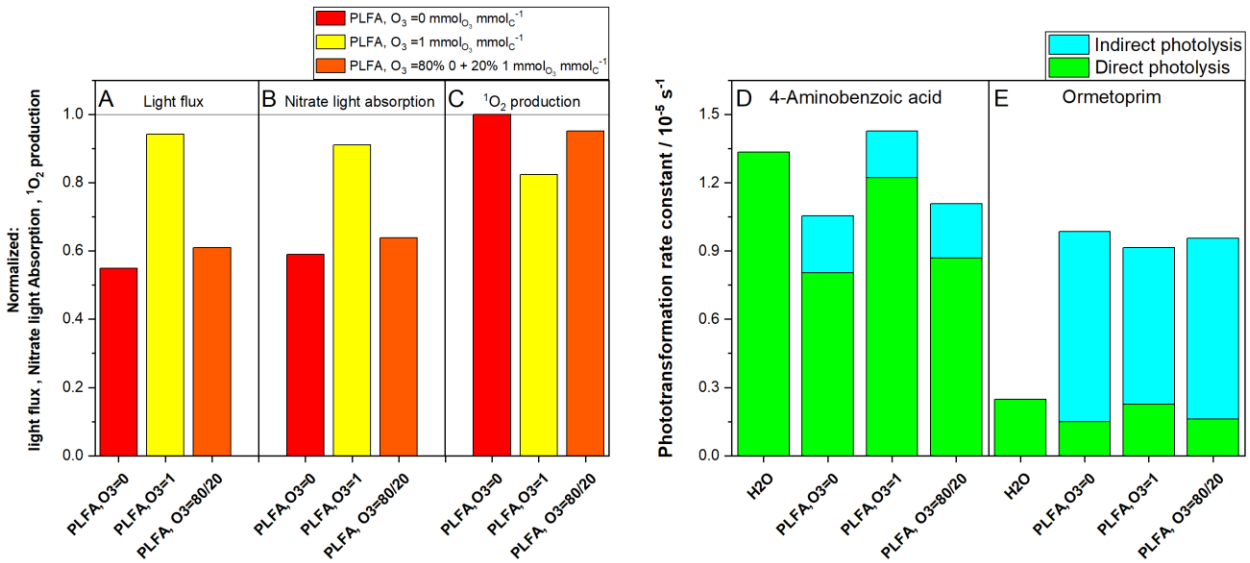

Figure 6. Results of the simple scenario (see main Text and Text S7, SI) on the effects of ozone on the photochemistry of a $5 mg_C\ L^{-1}$ PLFA solution, light path length = 1 m. (A) Normalized average photon fluence rate (290 – 400 nm) at 1 m path length (relative to ultrapure water). (B) Light absorption by nitrate (normalized to ultrapure water). (C) Singlet oxygen ($^1O_2$) production (normalized to non-ozonated PLFA). (D) and (E) Phototransformation rate constant of (D) 4-aminobenzoic acid and (E) ormetoprim in ultrapure water, non-ozonated, ozonated and a 80% non-ozonated +20% ozonated PLFA solution.

The Φ_{1O2} values for the studied natural water (SJR) ozonated in the presence of an $^{\bullet}OH$ scavenger follow the same trends as the two investigated model DOMs (Figures 3 and 5). However, in the absence of an $^{\bullet}OH$ scavenger Φ_{1O2} increases only moderately and a stronger decrease in light absorbance of SJR is observed. These observations indicate that for an ozonated water exposed to sunlight, $[^1O_2]_{ss}$ would probably decrease but that a stronger direct photolysis would be possible. Further investigations on the effects of ozonation in the absence of an $^{\bullet}OH$ scavenger are currently conducted to determine if the increase in Φ_{1O2} is also observed and to better assess the effects of an ozonation treatment step on the photophysical characteristics of a treated water.

Acknowledgements

Funding for this study came from the US National Science Foundation grant CBET #1453906 and through the University of Colorado Discovery Learning Apprenticeship. The authors would like to thank Anthony Kennedy for collecting the San Juan River sample.

Associated Content

Supporting information

The supporting information is available free of charge on the ACS website at DOI:

List of chemicals, analytical methods, experimental procedures, data treatment methods and additional texts, figures and tables

Author information

Corresponding author

*E-mail: Fernando.rosario@colorado.edu

ORCID

Frank Leresche: 0000-0001-8400-3142

Tyler Kurtz: 0000-0001-6310-3240

Garrett McKay: 0000-0002-6529-0892

Urs von Gunten: 0000-0001-6852-8977

Silvio Canonica: 0000-0001-6848-947X

Fernando Rosario-Ortiz: 0000-0002-3311-9089

Note

The authors declare no competing financial interest.

References

1. Fenner, K.; Canonica, S.; Wackett, L. P.; Elsner, M., Evaluating pesticide degradation in the environment: blind spots and emerging opportunities. *Science* **2013,** *341* (6147), 752-8.
2. Richard, C.; Canonica, S., Aquatic phototransformation of organic contaminants induced by coloured dissolved natural organic matter. In *Handbook of Environmental Chemistry*, Hutzinger, O., Ed. Springer-Verlag Berlin, Heidelberger Platz 3, D-14197 Berlin, Germany: 2005; Vol. 2, pp 299-323.
3. Vione, D.; Minella, M.; Maurino, V.; Minero, C., Indirect photochemistry in sunlit surface waters: photoinduced production of reactive transient species. *Chemistry* **2014,** *20* (34), 10590-606.
4. McNeill, K.; Canonica, S., Triplet state dissolved organic matter in aquatic photochemistry: reaction mechanisms, substrate scope, and photophysical properties. *Environ. Sci.: Processes Impacts* **2016,** *18* (11), 1381-1399.
5. Rosario-Ortiz, F. L.; Canonica, S., Probe Compounds to Assess the Photochemical Activity of Dissolved Organic Matter. *Environmental Science & Technology* **2016,** *50* (23), 12532-12547.
6. Hoigné, J.; Faust, B. C.; Haag, W. R.; Scully, F. E.; Zepp, R. G., Aquatic Humic Substances as Sources and Sinks of Photochemically Produced Transient Reactants. *Acs Symposium Series* **1989,** *219*, 363-381.
7. Boyle, E. S.; Guerriero, N.; Thiallet, A.; Del Vecchio, R.; Blough, N. V., Optical properties of humic substances and CDOM: relation to structure. *Environ. Sci. Technol.* **2009,** *43* (7), 2262-8.
8. Vaughan, P. P.; Blough, N. V., Photochemical formation of hydroxyl radical by constituents of natural waters. *Environ. Sci. Technol.* **1998,** *32* (19), 2947-2953.
9. Sun, L. N.; Qian, J. G.; Blough, N. V.; Mopper, K., Insights into the Photoproduction Sites of Hydroxyl Radicals by Dissolved Organic Matter in Natural Waters. *Environ. Sci. Technol. Lett.* **2015,** *2* (12), 352-356.
10. Boreen, A. L.; Arnold, W. A.; McNeill, K., Photochemical fate of sulfa drugs in the aquatic environment: sulfa drugs containing five-membered heterocyclic groups. *Environ. Sci. Technol.* **2004,** *38* (14), 3933-40.
11. Latch, D. E.; Stender, B. L.; Packer, J. L.; Arnold, W. A.; McNeill, K., Photochemical fate of pharmaceuticals in the environment: cimetidine and ranitidine. *Environ. Sci. Technol.* **2003,** *37* (15), 3342-50.
12. Kohn, T.; Grandbois, M.; McNeill, K.; Nelson, K. L., Association with natural organic matter enhances the sunlight-mediated inactivation of MS2 coliphage by singlet oxygen. *Environ. Sci. Technol.* **2007,** *41* (13), 4626-4632.
13. Kohn, T.; Nelson, K. L., Sunlight-mediated inactivation of MS2 coliphage via exogenous singlet oxygen produced by sensitizers in natural waters. *Environ. Sci. Technol.* **2007,** *41* (1), 192-197.
14. Nelson, K. L.; Boehm, A. B.; Davies-Colley, R. J.; Dodd, M. C.; Kohn, T.; Linden, K. G.; Liu, Y. Y.; Maraccini, P. A.; McNeill, K.; Mitch, W. A.; Nguyen, T. H.; Parker, K. M.; Rodriguez, R. A.; Sassoubre, L. M.; Silverman, A. I.; Wigginton, K. R.; Zepp, R. G., Sunlight-mediated inactivation of health-relevant microorganisms in water: a review of

mechanisms and modeling approaches. *Environ. Sci.: Processes Impacts* **2018,** *20* (8), 1089-1122.
15. Haag, W. R.; Hoigné, J.; Gassman, E.; Braun, A. M., Singlet Oxygen in Surface Waters .2. Quantum Yields of Its Production by Some Natural Humic Materials as a Function of Wavelength. *Chemosphere* **1984,** *13* (5-6), 641-650.
16. Maizel, A. C.; Li, J.; Remucal, C. K., Relationships Between Dissolved Organic Matter Composition and Photochemistry in Lakes of Diverse Trophic Status. *Environ. Sci. Technol.* **2017,** *51* (17), 9624-9632.
17. Dalrymple, R. M.; Carfagno, A. K.; Sharpless, C. M., Correlations between dissolved organic matter optical properties and quantum yield of singlet oxygen and hydrogen peroxide. *Environ. Sci. Technol.* **2010,** *44*, 5824-5829.
18. McKay, G.; Couch, K. D.; Mezyk, S. P.; Rosario-Ortiz, F. L., Investigation of the Coupled Effects of Molecular Weight and Charge-Transfer Interactions on the Optical and Photochemical Properties of Dissolved Organic Matter. *Environ. Sci. Technol.* **2016,** *50* (15), 8093-8102.
19. Zepp, R. G.; Schlotzhauer, P. F.; Sink, R. M., Photosensitized Transformations Involving Electronic-Energy Transfer in Natural-Waters - Role of Humic Substances. *Environ. Sci. Technol.* **1985,** *19* (1), 74-81.
20. Zhang, D.; Yan, S.; Song, W., Photochemically Induced Formation of Reactive Oxygen Species (ROS) from Effluent Organic Matter. *Environ. Sci. Technol.* **2014**, *48* (21) 12645-53.
21. Peterson, B. M.; McNally, A. M.; Cory, R. M.; Thoemke, J. D.; Cotner, J. B.; McNeill, K., Spatial and temporal distribution of singlet oxygen in Lake Superior. *Environ. Sci. Technol.* **2012,** *46* (13), 7222-9.
22. Sharpless, C. M., Lifetimes of triplet dissolved natural organic matter (DOM) and the effect of NaBH(4) reduction on singlet oxygen quantum yields: implications for DOM photophysics. *Environ. Sci. Technol.* **2012,** *46* (8), 4466-73.
23. Schmitt, M.; Erickson, P. R.; McNeill, K., Triplet-State Dissolved Organic Matter Quantum Yields and Lifetimes from Direct Observation of Aromatic Amine Oxidation. *Environ. Sci. Technol.* **2017,** *51* (22), 13151-13160.
24. Grebel, J. E.; Pignatello, J. J.; Mitch, W. A., Sorbic acid as a quantitative probe for the formation, scavenging and steady-state concentrations of the triplet-excited state of organic compounds. *Water Res.* **2011,** *45* (19), 6535-44.
25. Dong, M. M.; Rosario-Ortiz, F. L., Photochemical Formation of Hydroxyl Radical from Effluent Organic Matter. *Environ. Sci. Technol.* **2012,** *46* (7), 3788-3794.
26. Page, S. E.; Logan, J. R.; Cory, R. M.; McNeill, K., Evidence for dissolved organic matter as the primary source and sink of photochemically produced hydroxyl radical in arctic surface waters. *Environ. Sci.: Processes Impacts* **2014,** *16* (4), 807-822.
27. McKay, G.; Huang, W. X.; Romera-Castillo, C.; Crouch, J. E.; Rosario-Ortiz, F. L.; Jaffe, R., Predicting Reactive Intermediate Quantum Yields from Dissolved Organic Matter Photolysis Using Optical Properties and Antioxidant Capacity. *Environ. Sci. Technol.* **2017,** *51* (10), 5404-5413.
28. Lee, E.; Glover, C. M.; Rosario-Ortiz, F. L., Photochemical Formation of Hydroxyl Radical from Effluent Organic Matter: Role of Composition. *Environ. Sci. Technol.* **2013,** *47* (21), 12073-12080.

29. Coelho, C.; Guyot, G.; ter Halle, A.; Cavani, L.; Ciavatta, C.; Richard, C., Photoreactivity of humic substances: relationship between fluorescence and singlet oxygen production. *Environ. Chem. Lett.* **2010,** *9* (3), 447-451.
30. Sonntag, C.; Gunten, U., Chemistry of ozone in water and wastewater treatment: from basic principles to applications. IWA Publishing, London, UK, 2012.
31. Wenk, J.; Aeschbacher, M.; Salhi, E.; Canonica, S.; von Gunten, U.; Sander, M., Chemical oxidation of dissolved organic matter by chlorine dioxide, chlorine, and ozone: effects on its optical and antioxidant properties. *Environ. Sci. Technol.* **2013,** *47* (19), 11147-56.
32. Wenk, J.; Aeschbacher, M.; Sander, M.; von Gunten, U.; Canonica, S., Photosensitizing and Inhibitory Effects of Ozonated Dissolved Organic Matter on Triplet-Induced Contaminant Transformation. *Environ. Sci. Technol.* **2015,** *49* (14), 8541-9.
33. Phungsai, P.; Kurisu, F.; Kasuga, I.; Furumai, H., Changes in Dissolved Organic Matter Composition and Disinfection Byproduct Precursors in Advanced Drinking Water Treatment Processes. *Environ. Sci. Technol.* **2018,** *52* (6), 3392-3401.
34. Hammes, F.; Salhi, E.; Koster, O.; Kaiser, H. P.; Egli, T.; von Gunten, U., Mechanistic and kinetic evaluation of organic disinfection by-product and assimilable organic carbon (AOC) formation during the ozonation of drinking water. *Water Res.* **2006,** *40* (12), 2275-2286.
35. Wert, E. C.; Rosario-Ortiz, F. L.; Drury, D. D.; Snyder, S. A., Formation of oxidation byproducts from ozonation of wastewater. *Water Res.* **2007,** *41* (7), 1481-1490.
36. Onnby, L.; Salhi, E.; McKay, G.; Rosario-Ortiz, F. L.; von Gunten, U., Ozone and chlorine reactions with dissolved organic matter - Assessment of oxidant-reactive moieties by optical measurements and the electron donating capacities. *Water Res.* **2018,** (144), 64-75.
37. Dowideit, P.; von Sonntag, C., Reaction of ozone with ethene and its methyl- and chlorine-substituted derivatives in aqueous solution. *Environ. Sci. Technol.* **1998,** *32* (8), 1112-1119.
38. Ramseier, M. K.; von Gunten, U., Mechanisms of Phenol Ozonation-Kinetics of Formation of Primary and Secondary Reaction Products. *Ozone Sci. Engin.* **2009,** *31* (3), 201-215.
39. Tentscher, P. R.; Bourgin, M.; von Gunten, U., Ozonation of Para-Substituted Phenolic Compounds Yields p-Benzoquinones, Other Cyclic alpha,beta-Unsaturated Ketones, and Substituted Catechols. *Environ. Sci. Technol.* **2018,** *52* (8), 4763-4773.
40. Mvula, E.; von Sonntag, C., Ozonolysis of phenols in aqueous solution. *Org. Biomol. Chem.* **2003,** *1* (10), 1749-1756.
41. Hollender, J.; Zimmermann, S. G.; Koepke, S.; Krauss, M.; McArdell, C. S.; Ort, C.; Singer, H.; von Gunten, U.; Siegrist, H., Elimination of Organic Micropollutants in a Municipal Wastewater Treatment Plant Upgraded with a Full-Scale Post-Ozonation Followed by Sand Filtration. *Environ. Sci. Technol.* **2009,** *43* (20), 7862-7869.
42. Zimmermann, S. G.; Wittenwiler, M.; Hollender, J.; Krauss, M.; Ort, C.; Siegrist, H.; von Gunten, U., Kinetic assessment and modeling of an ozonation step for full-scale municipal wastewater treatment: Micropollutant oxidation, by-product formation and disinfection. *Water Res.* **2011,** *45* (2), 605-617.
43. Eggen, R. I.; Hollender, J.; Joss, A.; Scharer, M.; Stamm, C., Reducing the discharge of micropollutants in the aquatic environment: the benefits of upgrading wastewater treatment plants. *Environ. Sci. Technol.* **2014,** *48* (14), 7683-9.
44. Andreadakis, A. D., Wastewater treatment and disposal for the preservation of bathing and coastal water quality in touristic areas. *Marine Chem.* **1997,** *58* (3-4), 389-395.
45. Mostafa, S.; Rosario-Ortiz, F. L., Singlet oxygen formation from wastewater organic matter. *Environ. Sci. Technol.* **2013,** *47* (15), 8179-86.

46. Murphy, K. R.; Butler, K. D.; Spencer, R. G. M.; Stedmon, C. A.; Boehme, J. R.; Aiken, G. R., Measurement of Dissolved Organic Matter Fluorescence in Aquatic Environments: An Interlaboratory Comparison. *Environ. Sci. Technol.* **2010,** *44* (24), 9405-9412.
47. McKay, G.; Korak, J. A.; Erickson, P. R.; Latch, D. E.; McNeill, K.; Rosario-Ortiz, F. L., The Case Against Charge Transfer Interactions in Dissolved Organic Matter Photophysics. *Environ. Sci. Technol.* **2018,** *52* (2), 406-414.
48. Cawley, K. M.; Korak, J. A.; Rosario-Ortiz, F. L., Quantum Yields for the Formation of Reactive Intermediates from Dissolved Organic Matter Samples from the Suwannee River. *Environ. Engin. Sci.* **2015,** *32* (1), 31-37.
49. Weishaar, J. L.; Aiken, G. R.; Bergamaschi, B. A.; Fram, M. S.; Fujii, R.; Mopper, K., Evaluation of specific ultraviolet absorbance as an indicator of the chemical composition and reactivity of dissolved organic carbon. *Environ. Sci. Technol.* **2003,** *37* (20), 4702-4708.
50. Twardowski, M. S.; Boss, E.; Sullivan, J. M.; Donaghay, P. L., Modeling the spectral shape of absorption by chromophoric dissolved organic matter. *Marine Chem.* **2004,** *89* (1-4), 69-88.
51. Laszakovits, J. R.; Berg, S. M.; Anderson, B. G.; O'Brien, J. E.; Wammer, K. H.; Sharpless, C. M., p-Nitroanisole/Pyridine and p-Nitroacetophenone/Pyridine Actinometers Revisited: Quantum Yield in Comparison to Ferrioxalate. *Environ. Sci. Technol. Lett.* **2017,** *4* (1), 11-14.
52. Tentscher, P. R.; Bourgin, M.; von Gunten, U., Ozonation of Para-Substituted Phenolic Compounds Yields p-Benzoquinones, Other Cyclic alpha,beta-Unsaturated Ketones, and Substituted Catechols. *Environ. Sci. Technol.* **2018,** *52* (8), 4763-4773.
53. Ramseier, M. K.; von Gunten, U., Mechanisms of Phenol Ozonation-Kinetics of Formation of Primary and Secondary Reaction Products. *Ozone Sc. Eng.* **2009,** *31* (3), 201-215.
54. Hoigné, J.; Bader, H., Rate Constants of Reactions of Ozone with Organic and Inorganic-Compounds in Water. 2. Dissociation Organic-Coumpounds. *Water Res.* **1983,** *17* (2), 185-194.
55. Wilkinson, F.; Helman, W. P.; Ross, A. B., Quantum Yields for the Photosensitized Formation of the Lowest Electronically Excited Singlet-State of Molecular-Oxygen in Solution. *J. Phys. Chem. Ref. Data* **1993,** *22* (1), 113-262.
56. Kaur, R.; Anastasio, C., Light absorption and the photoformation of hydroxyl radical and singlet oxygen in fog waters. *Atmospheric Environ.* **2017,** *164*, 387-397.
57. Hallquist, M.; Wenger, J. C.; Baltensperger, U.; Rudich, Y.; Simpson, D.; Claeys, M.; Dommen, J.; Donahue, N. M.; George, C.; Goldstein, A. H.; Hamilton, J. F.; Herrmann, H.; Hoffmann, T.; Iinuma, Y.; Jang, M.; Jenkin, M. E.; Jimenez, J. L.; Kiendler-Scharr, A.; Maenhaut, W.; McFiggans, G.; Mentel, T. F.; Monod, A.; Prevot, A. S. H.; Seinfeld, J. H.; Surratt, J. D.; Szmigielski, R.; Wildt, J., The formation, properties and impact of secondary organic aerosol: current and emerging issues. *Atmospheric Chem. and Phys.* **2009,** *9* (14), 5155-5236.
58. Peuravuori, J.; Pihlaja, K., Molecular size distribution and spectroscopic properties of aquatic humic substances. *Analytica Chimica Acta* **1997,** *337* (2), 133-149.
59. Maizel, A. C.; Remucal, C. K., Molecular Composition and Photochemical Reactivity of Size-Fractionated Dissolved Organic Matter. *Environ. Sci. Technol.* **2017,** *51* (4), 2113-2123.
60. Turro, N. J.; Ramamurthy, V.; Scaiano, J. C., *Modern Molecular Photochemistry of Organic Molecules*. University of California: Sausalito, California, 2010.

61. Klán, P.; Wirz, J., *Photochemistry of Organic Compounds: From Concepts to Practice*. John Wiley & Sons, 2009.
62. Kasha, M., Characterization of Electronic Transitions in Complex Molecules. *Discussions of the Faraday Society* **1950,** (9), 14-19.
63. Buffle, M. O.; Schumacher, J.; Meylan, S.; Jekel, M.; von Gunten, U., Ozonation and advanced oxidation of wastewater: Effect of O-3 dose, pH, DOM and HO center dot-scavengers on ozone decomposition and HO center dot generation. *Ozone Sci. Engin.* **2006,** *28* (4), 247-259.
64. Leresche, F.; von Gunten, U.; Canonica, S., Probing the Photosensitizing and Inhibitory Effects of Dissolved Organic Matter by Using N,N-dimethyl-4-cyanoaniline (DMABN). *Environ. Sci. Technol.* **2016,** *50* (20), 10997-11007.